Particle-hole calculation of the longitudinal response function of ^{12}C

A. Dellafiore,* F. Lenz, and F. A. Brieva†
Swiss Institute for Nuclear Research, 5234 Villigen, Switzerland
(Received 13 November 1984)

The longitudinal response function of ^{12}C in the range of momentum transfers 200 MeV/$c \leq q \leq$ 550 MeV/c is calculated in the Tamm-Dancoff approximation. The particle-hole Green's function is evaluated by means of a doorway-state expansion. This method allows us to take into account finite-range residual interactions in the continuum, including exchange processes. At low momentum transfers, calculations agree qualitatively with the data. The data cannot be reproduced at momentum transfers around 450 MeV/c. This discrepancy can be accounted for neither by uncertainties in the residual interaction, nor by more complicated processes in the nuclear final states.

I. INTRODUCTION

Quasielastic electron scattering at high energy and momentum transfer is dominated by the single-particle degrees of freedom of nuclei. The first systematic experimental results have been successfully described within the nuclear Fermi-gas model.[1] More recent experiments,[2] which allow for a separation of the cross section into longitudinal and transverse response functions, indicate the importance of processes which are beyond such a simple picture.

Extensions of this model by using realistic single-particle wave functions and allowing for final state interaction of the knocked-out nucleon do not qualitatively improve the agreement with the data, as illustrated in Fig. 1 for the longitudinal response functions of ^{12}C and ^{40}Ca.

Discrepancies between theory and experiment in the region of the quasielastic peak are particularly disturbing. This is especially true for the longitudinal response. As shown in Ref. 3, final state interaction effects cannot be responsible for these discrepancies unless our understanding of the nucleon-nucleus interaction at the corresponding energies is qualitatively incorrect. Furthermore, contrary to the transverse response, neither meson exchange corrections nor virtual isobar excitation are expected to be important for the longitudinal response. Indeed, the measured longitudinal structure function is very small for energies above the quasielastic peak, while on the contrary the transverse structure function exhibits appreciable strength in the region between quasielastic and Δ peaks.

In the absence of any obvious explanation, these discrepancies have stimulated interpretations in terms of relativistic effects[4] or modifications of the nucleonic structure.[5] The possibility of learning about such fundamental aspects of nuclear physics from the study of quasielastic scattering is very appealing. However, the treatment of the more standard many-body dynamics in the quasielastic process is not sufficient to rule out *a priori* deviations from the single-particle description of the order of 20%.

In this paper we explore the importance of these many-body effects by investigating the contribution of particle-hole rescattering to the longitudinal response in the quasielastic region. These processes are well known to be important at smaller energy and momentum transfers: particle-hole rescattering is one of the mechanisms which concentrates strength in low-lying collective states. However, in extending the calculation of these processes from discrete excitations to the quasielastic region, we have to keep in mind the changes in the kinematics. The much larger momentum transfer involved requires one to account for finite range effects in the particle-hole force. The much larger energy transfer, on the other hand, makes a description of particle propagation in terms of the nuclear ground state potential insufficient. Rather a

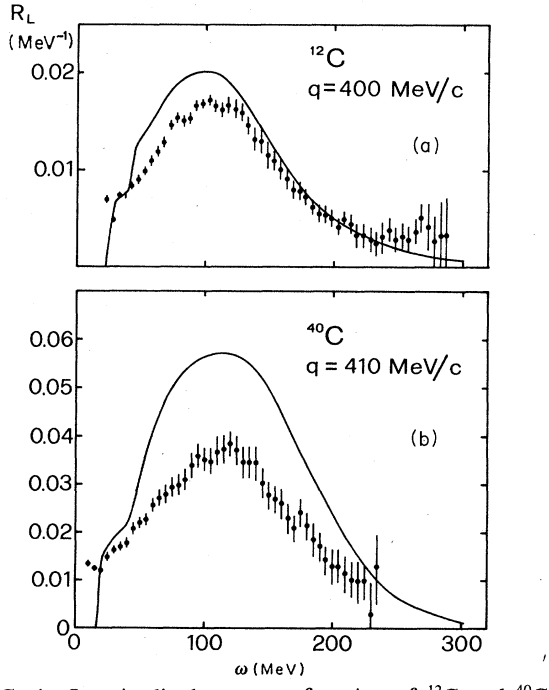

FIG. 1. Longitudinal response function of ^{12}C and ^{40}Ca at constant momentum transfer. The curves are calculated in the independent-particle model of Ref. 3; the data are from Refs. 2 and 6.

description in terms of the optical potential is required. At the same time we have to expect an energy dependence of the residual particle-hole force coming from the energy dependence of the (in-medium) N-N interaction which is the origin of both the optical potential and this residual force.

The technical difficulties encountered in performing such a calculation are related to the necessity of accounting simultaneously for the particle propagation in the continuum and the finite range in the particle-hole force. This required a new method for solving the corresponding equation for the polarization propagator. In the method which we employ the polarization propagator is calculated in a doorway-state expansion. This method neither requires discretization of the continuum nor truncation to a subspace of the 1p-1h space. Moreover, it allows for a description of discrete excitations, giant resonances, and quasielastic scattering on an equal footing.

In our calculations we use parametrizations of the residual interaction which have been determined from low energy nuclear structure studies.

We have not been able to circumvent the difficulties associated with the energy dependence of the residual interaction. In principle, a model is needed which provides energy and momentum dependences of both the optical potential and the residual force. For the optical potential, both theoretical calculations and phenomenological parametrizations are available. For the residual interaction, on the contrary, no such information exists. For this reason we are not able to predict, for high momentum transfer, the detailed distribution of the strength as a function of the excitation energy. However our results provide the scale for the importance of these many-body corrections to quasielastic scattering.

II. LONGITUDINAL SINGLE-PARTICLE RESPONSE

The starting point for our investigation is the longitudinal response function in the independent-particle model. We define this response function by

$$S(q,\omega)=-\frac{1}{\pi}\mathrm{Im}\Pi^0(q,\omega) \tag{2.1}$$

(in Appendix A we give a slightly different definition including form factors for the sake of comparison with experimental data).

The quantity $\Pi^0(q,\omega)$ is the polarization propagator in the independent-particle model and is given by[3]

$$\Pi^0(q,\omega)=\sum_i \langle 0 \mid O^\dagger(i)G(i)O(i) \mid 0\rangle \ , \tag{2.2a}$$

with

$$O(i)=\mid i^{-1}\rangle \left[\frac{1+\tau_i^3}{2}e^{i(A-1/A)\mathbf{q}\cdot\mathbf{y}_i}+F_{A-1}(q)\right] \times\left[\frac{A}{2}-\frac{1+\tau_i^3}{2}\right]e^{-i(1/A)\mathbf{q}\cdot\mathbf{y}_i}\Bigg]\langle i^{-1}\mid \ . \tag{2.2b}$$

The operator (2.2b) approximatively accounts for the c.m. correction to the standard operator

$$\frac{1+\tau_i^3}{2}e^{i\mathbf{q}\cdot\mathbf{x}_i} \ .$$

The detailed derivation of this form of the operator and a discussion of its validity are given in Appendix B. Here we only note that it eliminates completely the giant isoscalar dipole c.m. excitation at small momentum transfers. Equation (2.2b) might thus be interpreted as a momentum-transfer dependent effective charge operator.

The hole wave functions (φ_i) are generated in a Woods-Saxon potential and the Green's function $G(i)$ is given by

$$G(i)=\mid i^{-1}\rangle\left[\omega_i-\frac{q^2}{2Am}-\frac{P_i^2}{2\mu} -V_C(i)-U(i)\right]^{-1}\langle i^{-1}\mid \ , \tag{2.2c}$$

with

$$\omega_i=\omega-\epsilon_i$$

and ϵ_i are the hole energies, m the nucleon mass, and μ the reduced mass

$$\mu=\frac{A-1}{A}m \ .$$

$V_C(i)$ and $U(i)$ are the Coulomb and optical potentials, respectively.[3]

In Fig. 1 we show the calculated longitudinal response functions for ^{12}C and ^{40}Ca at $q=400$ and 410 MeV/c, respectively, in comparison with experimental data. This calculation differs from that of Ref. 3 only by some details like the use of the modified operator (2.2b) and of Woods-Saxon rather than harmonic oscillator hole wave functions.

As mentioned in the Introduction, we observe severe discrepancies between theory and experiment in the quasielastic region. We emphasize the importance of the separation of the response into longitudinal and transverse terms. In fact, the summed cross section agrees very well with the predictions of Ref. 3 in the quasielastic peak region (the data shown in Fig. 8 of Ref. 3 were only preliminary, the final data[7] agree with the calculation). Obviously, this implies that this independent particle model underestimates by the same amount the transverse response.

III. PARTICLE-HOLE RESCATTERING IN THE LONGITUDINAL RESPONSE

In this section we derive the basic formulae to calculate the particle-hole rescattering contribution to the response function. We define the polarization propagator corresponding to $\Pi^0(q,\omega)$ of Eq. (2.2a) in the particle coordinate space by

$$\Pi^0_{\alpha'\alpha}(\mathbf{r}',\mathbf{r})=\sum_i \mid i^{-1}\rangle G_{\alpha'\alpha}(\mathbf{r}',\mathbf{r},\omega_i)\langle i^{-1}\mid \ , \tag{3.1}$$

which describes the propagation of a particle from $\mathbf{r}$ to $\mathbf{r}'$

in the presence of a hole state $|i^{-1}\rangle$. The indexes α,α' denote the spin and isospin quantum numbers of the particle (due to the spin-orbit interaction in the optical potential, G is nondiagonal in the spin projection).

To lowest order in the particle-hole interaction V the polarization propagator is given by[8]

$$\Pi_{\alpha'\alpha}(\mathbf{r}',\mathbf{r})\approx\Pi^0_{\alpha'\alpha}(\mathbf{r}',\mathbf{r})+\sum_{ij\beta\beta'}|j^{-1}\rangle\int d\mathbf{r}_1 d\mathbf{r}_2[\,G_{\alpha'\beta'}(\mathbf{r}',\mathbf{r}_1,\omega_j)\varphi_i^\dagger(\mathbf{r}_2)V_{\beta'\beta}(\mathbf{r}_1,\mathbf{r}_2)\varphi_j(\mathbf{r}_1)G_{\beta\alpha}(\mathbf{r}_2,\mathbf{r},\omega_i)$$
$$-G_{\alpha'\beta'}(\mathbf{r}',\mathbf{r}_2,\omega_j)\varphi_i^\dagger(\mathbf{r}_1)V_{\beta'\beta}(\mathbf{r}_1,\mathbf{r}_2)\varphi_j(\mathbf{r}_1)G_{\beta\alpha}(\mathbf{r}_2,\mathbf{r},\omega_i)]\langle i^{-1}|\ . \tag{3.2}$$

Here we have assumed V to be a local interaction. In the actual calculation we have used the following form:

$$V(1,2)=V(\mathbf{r}_1-\mathbf{r}_2)(a_0+a_1P_\sigma+a_2P_\tau+a_3P_\sigma P_\tau)\ . \tag{3.3a}$$

The coefficients a_i determine the relative weight of the various spin and isospin exchange operators. In Eq. (3.2), $V_{\beta'\beta}$ is the matrix element of $V(1,2)$ in the spin-isospin space of the particle. The local interaction V is assumed to be of the form

$$V(\mathbf{x})=V_0\frac{e^{-\mu x}}{\mu x}\ . \tag{3.3b}$$

In Fig. 2 we show the diagrams corresponding to the various terms in Eq. (3.2). This representation makes transparent the difficulties associated with the evaluation of the last (exchange) term in Eq. (3.2). Unlike the direct one, the exchange term does not involve the particle propagator and the hole wave function at the same point in coordinate space. Only by neglecting the exchange term, as is done in the ring approximation, or by assuming the particle-hole force to be of zero range, the obvious technical complications associated with the presence of the exchange term do not occur. In the application to quasielastic electron scattering at large momentum transfer neither of these two simplifications is appropriate. In our approach the direct and the exchange term are treated on equal footing.

The structure of Eq. (3.2) suggest introducing the "wave operator" Ω^0:

$$\Omega^0_{\alpha\beta}(\mathbf{r}',\mathbf{r}_2)=\sum_{ij\beta'}|j^{-1}\rangle\int d\mathbf{r}_1[G_{\alpha\beta'}(\mathbf{r}',\mathbf{r}_1,\omega_j)\varphi_i^\dagger(\mathbf{r}_2)V_{\beta'\beta}(\mathbf{r}_1,\mathbf{r}_2)\varphi_j(\mathbf{r}_1)-G_{\alpha\beta'}(\mathbf{r}',\mathbf{r}_2,\omega_j)\varphi_i^\dagger(\mathbf{r}_1)V_{\beta'\beta}(\mathbf{r}_1,\mathbf{r}_2)\varphi_j(\mathbf{r}_1)]\langle i^{-1}|\ . \tag{3.4}$$

In terms of Ω^0, Eq. (3.2) is written as an operator equation

$$\hat{\Pi}\approx(1+\hat{\Omega}^0)\hat{\Pi}^0\ . \tag{3.5}$$

Successive iterations of the residual interaction in the particle-hole space are obtained from repeated applications of the wave operator $\hat{\Omega}^0$. The resulting polarization propagator $\hat{\Pi}$ therefore satisfies the equation

$$\hat{\Pi}=\hat{\Pi}^0+\hat{\Omega}^0\hat{\Pi}\ , \tag{3.6a}$$

which has the formal solution

$$\hat{\Pi}=\frac{1}{1-\hat{\Omega}^0}\hat{\Pi}^0\ . \tag{3.6b}$$

The polarization propagator $\Pi(q,\omega)$ corresponding to the particle-hole propagator $\hat{\Pi}$ of Eq. (3.6b) is given by [cf. Eq. (2.2a)]

$$\Pi(q,\omega)=\sum_{\substack{ij\\ \alpha\alpha'}}\int d\mathbf{r}\,d\mathbf{r}'\langle\varphi_j|O^\dagger(j)|\mathbf{r}',\boldsymbol{\alpha}'\rangle\langle j^{-1}|\Pi_{\alpha'\alpha}(\mathbf{r}',\mathbf{r})|i^{-1}\rangle\langle\mathbf{r},\alpha|O(i)|\varphi_i\rangle$$
$$=\sum_{ij}\langle 0|O^\dagger(j)\frac{1}{1-\hat{\Omega}^0}\hat{\Pi}^0O(i)|0\rangle\ . \tag{3.7}$$

In our approach the inversion of the operator $(1-\hat{\Omega}^0)$ is achieved in a doorway-state expansion.[9] We introduce the doorway states

$$\langle D^0|=(N^0)^{-1}\sum_i\langle 0|O^\dagger(i) \tag{3.8a}$$

and

$$|\tilde{D}^0\rangle=(\tilde{N}^0)^{-1}\hat{\Pi}^0\sum_i O(i)|0\rangle\ . \tag{3.8b}$$

The interpretation of these doorway states is straightforward. The state $|D^0\rangle$ is the coherent superposition of the particle-hole states formed by the absorption of the incident photon, while $|\tilde{D}^0\rangle$, in addition, contains the spreading of this coherent particle-hole state due to the propagation of the system after the absorption of the photon.

The single-particle response determines the normalization of the doorway states. The requirement

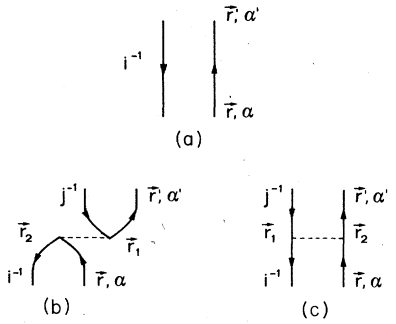

FIG. 2. Diagrams corresponding to the first (a), second (b), and third (c) terms on the right-hand side of Eq. (3.2). The diagram (a) represents the independent-particle model polarization propagator (3.1). Diagram (b) corresponds to the direct particle-hole interaction, while diagram (c) is the exchange term.

$$\langle D^0 | \tilde{D}^0 \rangle = 1 , \tag{3.9a}$$

in fact, implies

$$N^0 \tilde{N}^0 = \Pi^0(q,\omega) . \tag{3.9b}$$

Starting from $\langle D^0 |$ and $| \tilde{D}^0 \rangle$, a biorthogonal basis is constructed by repeated application of the wave operator $\hat{\Omega}^0$. The recurrence relations are

$$N^k \langle D^k | = \langle D^{k-1} | \hat{\Omega}^0 - \sum_{j=0}^{k-1} \langle D^j | \langle D^{k-1} | \hat{\Omega}^0 | \tilde{D}^j \rangle , \tag{3.10a}$$

$$\tilde{N}^k | \tilde{D}^k \rangle = \hat{\Omega}^0 | \tilde{D}^{k-1} \rangle - \sum_{j=0}^{k-1} | \tilde{D}^j \rangle \langle D^j | \hat{\Omega}^0 | \tilde{D}^{k-1} \rangle , \tag{3.10b}$$

and the normalization conditions

$$\langle D^k | \tilde{D}^k \rangle = 1$$

are imposed.

In this doorway-state basis the operator $\hat{\Omega}^0$ is, by construction, tridiagonal. The matrix element (3.7) can therefore be represented in terms of a continued fraction:

$$\Pi(q,\omega) = \frac{\Pi^0(q,\omega)}{1 - \Omega^0_{00} - \dfrac{\Omega^0_{01}\Omega^0_{10}}{1 - \Omega^0_{11} - \cdots}} \tag{3.11a}$$

with

$$\Omega^0_{jk} = \langle D^j | \hat{\Omega}^0 | \tilde{D}^k \rangle . \tag{3.11b}$$

We illustrate this procedure in the case of infinite nuclear matter. Because of momentum conservation it is appropriate to use the momentum representation of the various quantities. From the definitions (3.1), (3.4), and (3.8), we obtain (for isoscalar response and Wigner interaction)

$$\langle D^0 | = (N^0)^{-1} \int d\mathbf{k} \langle \mathbf{k}+\mathbf{q}, \mathbf{k}^{-1} | , \tag{3.12a}$$

$$\hat{\Pi}^0 = \int d\boldsymbol{\kappa}\, d\mathbf{k} \frac{| \boldsymbol{\kappa}, \mathbf{k}^{-1} \rangle \langle \boldsymbol{\kappa}, \mathbf{k}^{-1} |}{\omega^+ + \dfrac{k^2}{2m} - \dfrac{\kappa^2}{2m}} , \tag{3.12b}$$

$$\hat{\Omega}^0 = \int d\mathbf{k}\, d\mathbf{k}'\, d\boldsymbol{\kappa}\, d\boldsymbol{\kappa}' \frac{1}{\omega^+ + \dfrac{k'^2}{2m} - \dfrac{\kappa'^2}{2m}} \delta[\boldsymbol{\kappa}' - (\mathbf{k}' - \mathbf{k} + \boldsymbol{\kappa})][V(\boldsymbol{\kappa} - \mathbf{k}) - \tfrac{1}{4} V(\mathbf{k}' - \mathbf{k})] | \boldsymbol{\kappa}' \mathbf{k}'^{-1} \rangle \langle \boldsymbol{\kappa}, \mathbf{k}^{-1} | . \tag{3.12c}$$

Here, $\boldsymbol{\kappa}$ and $\boldsymbol{\kappa}'$ are particle momenta, $\mathbf{k}$ and $\mathbf{k}'$ hole momenta; the momentum integrals are understood to be above or below the Fermi surface and to include the sum over spin and isospin indexes.

In order to construct the next doorway state and to calculate Ω^0_{00} we need to evaluate $\langle D^0 | \hat{\Omega}^0$. Using the above-mentioned definitions, we immediately obtain

$$\begin{aligned} \langle D^0 | \hat{\Omega}^0 &= (N^0)^{-1} \int d\mathbf{p}\, d\mathbf{k} \frac{1}{\omega^+ + \dfrac{p^2}{2m} - \dfrac{(\mathbf{p}+\mathbf{q})^2}{2m}} [V(\mathbf{q}) - \tfrac{1}{4} V(\mathbf{p}-\mathbf{k})] \langle \mathbf{k}+\mathbf{q}, \mathbf{k}^{-1} | \\ &= \Pi^0(q,\omega) V(q) \langle D^0 | - (N^0)^{-1} \int d\mathbf{p}\, d\mathbf{k} \frac{1}{\omega^+ + \dfrac{p^2}{2m} - \dfrac{(\mathbf{p}+\mathbf{q})^2}{2m}} \tfrac{1}{4} V(\mathbf{p}-\mathbf{k}) \langle \mathbf{k}+\mathbf{q}, \mathbf{k}^{-1} | . \end{aligned} \tag{3.13}$$

It is now easy to see how, in this doorway-state formalism, the simple result of the ring approximation emerges. Neglecting the second term in Eq. (3.13), which arises from the exchange process, makes $\langle D^0 | \hat{\Omega}^0$ parallel to $\langle D^0 |$ and therefore [cf. Eq. (3.10a)]

$$N^1 \langle D^1 | = \Pi^0(q,\omega) V(q) [\langle D^0 | - \langle D^0 | \tilde{D}^0 \rangle \langle D^0 |] = 0 \tag{3.14a}$$

because of the normalization condition (3.9a).

Consequently the continued fraction (3.11a) becomes

$$\Pi(q,\omega)=\frac{\Pi^0(q,\omega)}{1-V(q)\Pi^0(q,\omega)}\ , \tag{3.14b}$$

i.e., in this case the doorway approximation is exact.

If we keep the exchange term, but stop the doorway-state expansion at lowest order, we get

$$\Pi(q,\omega)\approx\frac{\Pi^0(q,\omega)}{1-\tilde{V}(q)\Pi^0(q,\omega)} \tag{3.15a}$$

with

$$\tilde{V}(q)=V(q)-\tfrac{1}{4}V_{\rm ex}(q,\omega)\ . \tag{3.15b}$$

The exchange contribution is given by

$$V_{\rm ex}(q,\omega)=\frac{\int d\mathbf{p}\,d\mathbf{k}\dfrac{V(\mathbf{p}-\mathbf{k})}{\left[\omega^+-\dfrac{(\mathbf{p}+\mathbf{q})^2}{2m}+\dfrac{p^2}{2m}\right]\left[\omega^+-\dfrac{(\mathbf{k}+\mathbf{q})^2}{2m}+\dfrac{k^2}{2m}\right]}}{\int d\mathbf{p}\,d\mathbf{k}\dfrac{1}{\left[\omega^+-\dfrac{(\mathbf{p}+\mathbf{q})^2}{2m}+\dfrac{p^2}{2m}\right]\left[\omega^+-\dfrac{(\mathbf{k}+\mathbf{q})^2}{2m}+\dfrac{k^2}{2m}\right]}}\ . \tag{3.15c}$$

Of course, an exact treatment of the exchange term leads to a continued fraction expansion of infinite order even in nuclear matter.

As it is evident from Eqs. (3.15), the particle-hole force enters the direct and exchange terms in different ways. While the direct process is given in terms of the residual interaction at the momentum transfer corresponding to the external photon, the momentum-transfer dependence of the residual interaction in the exchange term is controlled entirely by the nucleon momenta in the ground state. This is a consequence of momentum conservation in direct and exchange processes (see Fig. 2).

In calculating the response function for finite nuclei, we use a partial-wave decomposition of the polarization propagator and evaluate the contribution of each partial wave in the doorway-state formalism. Here the doorway states are coherent superpositions of particle-hole states formed by the absorption of a photon with definite multipolarity rather than definite momentum. The lowest partial-wave doorway states are defined by

$$N^0\langle D^0\,|\,\mathbf{r}\rangle=4\pi\sum_{LM}(-i)^L Y_{LM}(\hat{\mathbf{q}})N_L^0\langle D_{LM}^0\,|\,\mathbf{r}\rangle\ , \tag{3.16a}$$

$$\tilde{N}^0\langle\mathbf{r}\,|\,\tilde{D}^0\rangle=4\pi\sum_{LM}(i)^L Y_{LM}^*(\hat{\mathbf{q}})\tilde{N}_L^0\langle\mathbf{r}\,|\,\tilde{D}_{LM}^0\rangle\ . \tag{3.16b}$$

From Eqs. (3.8) we obtain the following explicit form of the partial-wave doorway states:

$$N_L^0\langle D_{LM}^0\,|\,\mathbf{r}\rangle=\sum_i\sum_{j_\alpha l_\alpha}\langle\tau_i\,|\,j_L(qr)\frac{u_i(r)}{r}\times[X_{\alpha i}^{LM}(\hat{\mathbf{r}})]^\dagger\langle i^{-1}|\ , \tag{3.17a}$$

$$\tilde{N}_L^0\langle\mathbf{r}\,|\,\tilde{D}_{LM}^0\rangle=\sum_i\sum_{j_\alpha l_\alpha}|\,i^{-1}\rangle\int_0^\infty dx\frac{1}{r}g^{j_\alpha l_\alpha}(r,x,\omega_i)\times j_L(qx)u_i(x)X_{\alpha i}^{LM}(\hat{\mathbf{r}})\,|\,\tau_i\rangle\ . \tag{3.17b}$$

The radial dependence of $\langle D_{LM}^0\,|$ contains the Bessel function corresponding to the absorbed photon and the radial hole wave function u_i (here for simplicity we have neglected the c.m. corrections). The definitions (3.16) and (3.17) are appropriate for the isoscalar response, therefore the isospin dependence of the doorway states is described by the hole isospinor $|\,\tau_i\rangle$. The angular and spin dependences are factorized in the functions

$$X_{\alpha i}^{LM}(\hat{\mathbf{r}})=\sum_{m_\alpha}\mathscr{Y}_{j_\alpha l_\alpha}^{m_\alpha}(\hat{\mathbf{r}})R_{\alpha i}^{LM} \tag{3.18a}$$

with

$$R_{\alpha i}^{LM}=\int d\hat{\mathbf{x}}[\mathscr{Y}_{j_\alpha l_\alpha}^{m_\alpha}(\hat{\mathbf{x}})]^\dagger\mathscr{Y}_{j_i l_i}^{m_i}(\hat{\mathbf{x}})Y_{LM}(\hat{\mathbf{x}}) \tag{3.18b}$$

which contain the coupling of particle (j_α,l_α) and hole (j_i,l_i) angular momenta to the incident photon angular momentum (L). The angular integral is easily expressed in terms of 3-j symbols.

The associated doorway state $|\,\tilde{D}_{LM}^0\rangle$ contains in addition the (partial-wave projected) particle-hole propagator Π^0 [cf. Eq. (3.8b)]. This propagator is diagonal in the hole quantum numbers and the particle propagation is described by the radial Green's function

$$\frac{1}{rr'}g^{j_\alpha l_\alpha}(r',r,\omega_i)$$

which is the partial-wave projection of the propagator (2.2c).

The wave operator of Eq. (3.4) contains a direct and an exchange term. We therefore define

$$\langle\tau_\beta|\,\Omega^0(\mathbf{r}',\mathbf{r})\,|\,\tau_\alpha\rangle=\langle\tau_\beta|\,\Delta(\mathbf{r}',\mathbf{r})-E(\mathbf{r}',\mathbf{r})\,|\,\tau_\alpha\rangle\ , \tag{3.19}$$

where $\tau_{\alpha,\beta}$ denotes the particle isospin component. The partial-wave decomposition of Δ and E then reads

$$\langle\tau_\beta|\Delta(\mathbf{r}',\mathbf{r})|\tau_\alpha\rangle=4\pi\sum_{ij}|j^{-1}\rangle\delta_{\tau_\alpha\tau_i}\delta_{\tau_\beta\tau_j}\sum_{\substack{j_\alpha l_\alpha\\ j_\beta l_\beta}}\sum_{lm}\int_0^\infty dx\frac{1}{r'}g^{j_\beta l_\beta}(r',x,\omega_j)u_j(x)v_l(x,r)\frac{u_i(r)}{r}[X^{lm}_{\alpha i}(\hat{\mathbf{r}})]^\dagger X^{lm}_{\beta j}(\hat{\mathbf{r}}')\langle i^{-1}| \tag{3.20a}$$

and

$$\langle\tau_\beta|E(\mathbf{r}',\mathbf{r})|\tau_\alpha\rangle=4\pi\sum_{ij}|j^{-1}\rangle\delta_{\tau_\alpha\tau_\beta}\delta_{\tau_i\tau_j}\sum_{\substack{j_\alpha l_\alpha\\ j_\beta l_\beta}}\sum_{lm}\frac{1}{rr'}g^{j_\beta l_\beta}(r',r,\omega_j)\int_0^\infty dx\,u_j(x)u_i(x)v_l(x,r)$$
$$\times\sum_{m_\beta}[X^{lm}_{\alpha\beta}(\hat{\mathbf{r}})]^\dagger\mathscr{Y}^{m_\beta}_{j_\beta l_\beta}(\hat{\mathbf{r}}')R^{lm}_{ji}\langle i^{-1}|\ . \tag{3.20b}$$

For simplicity, again we have kept here only the Wigner term in the particle-hole interaction, v_l is the multipole component of this interaction

$$V(\mathbf{x}-\mathbf{x}')=4\pi\sum_{lm}v_l(x,x')Y_{lm}(\hat{\mathbf{x}})Y^*_{lm}(\hat{\mathbf{x}}')\ . \tag{3.20c}$$

The partial-wave decomposed operator (3.20) can now be applied to the partial-wave doorway-state (3.17) and the higher (partial-wave) doorway states are generated according to the recursion relations (3.10). In this way we obtain the continued fraction representation for each multipole component.

In applying the wave operator to the doorway states, through the angular integrations over the X functions we obtain the selection rules for direct and exchange particle-hole scattering. The integrals involved when applying the direct term (3.20a) of the wave operator are

$$\sum_{m_i}\int d\hat{\mathbf{x}}[X^{lm}_{\beta i}(\hat{\mathbf{x}})]^\dagger X^{LM}_{\alpha i}(\hat{\mathbf{x}})=\sum_{m_i m_\alpha}R^{lm}_{\alpha i}R^{LM}_{\alpha i}=\delta_{l,L}\delta_{m,M}\frac{(2j_\alpha+1)(2j_i+1)}{4\pi(2L+1)}\langle j_\alpha j_i-\tfrac{1}{2}\tfrac{1}{2}|L0\rangle^2\ , \tag{3.21a}$$

and, when applying the exchange part (3.20b) of the wave operator

$$\sum_{\substack{m_i m_p\\ m}}Y^{m_\beta}_{j_\beta l_\beta}(\hat{\mathbf{r}}')R^{lm}_{ij}\int d\hat{\mathbf{x}}[X^{lm}_{\alpha\beta}(\hat{\mathbf{x}})]^\dagger X^{LM}_{\alpha i}(\hat{\mathbf{x}})=\sum_{\substack{m_i m_\alpha\\ m_\beta m}}\mathscr{Y}^{m_\beta}_{j_\beta l_\beta}(\hat{\mathbf{r}}')R^{lm}_{ij}R^{lm}_{\alpha\beta}R^{LM}_{\alpha i}$$
$$=X^{LM}_{\beta j}(\hat{\mathbf{r}}')(-1)^{l+L+1}\frac{(2j_\alpha+1)(2j_i+1)}{4\pi}\begin{Bmatrix}j_\beta & j_j & L\\ j_i & j_\alpha & l\end{Bmatrix}$$
$$\times\frac{\langle j_\alpha j_i-\frac{1}{2}\frac{1}{2}|L0\rangle\langle j_\beta j_\alpha-\frac{1}{2}\frac{1}{2}|l0\rangle\langle j_i j_j-\frac{1}{2}\frac{1}{2}|l0\rangle}{\langle j_\beta j_j-\frac{1}{2}\frac{1}{2}|L0\rangle}\ . \tag{3.21b}$$

By construction, the application of the wave operator reproduces the angular dependence of the doorway states as contained in the X functions [cf. Eqs. (3.17) and (3.18)].

In analogy with the nuclear matter result we recognize the different angular-momentum dependence of the residual interaction in direct and exchange particle-hole rescattering. As follows from angular-momentum conservation, the multipolarity of the interaction in the direct term is that of the incident photon, while in the exchange term the allowed multipolarities are determined by the hole angular momenta [expressed in the 6-j symbol of Eq. (3.21b)].

The formalism is straightforwardly extended to include the more general form (3.3a) of the interaction, the c.m. corrections, and the isospin dependence of the transition operator (2.2b). Detailed formulae are presented in Appendix C.

IV. NUCLEAR MATTER ESTIMATES

We first discuss the main characteristics of the effects of the particle-hole rescattering process in the longitudinal response function. We start this discussion assuming a spin-isospin independent interaction, i.e., we take

$$a_0=1,\ a_1=a_2=a_3=0 \tag{4.1a}$$

in Eq. (3.3a). The strength and range parameters are chosen according to the standard parametrization of the residual interaction[10]

$$V_0=-36\ \text{MeV},\ \ \mu=0.714\ \text{fm}^{-1}\ . \tag{4.1b}$$

Figure 3 shows the modification of the isoscalar longitudinal response function for ^{12}C due to particle-hole rescattering. Figure 3(a) displays separately the effects of

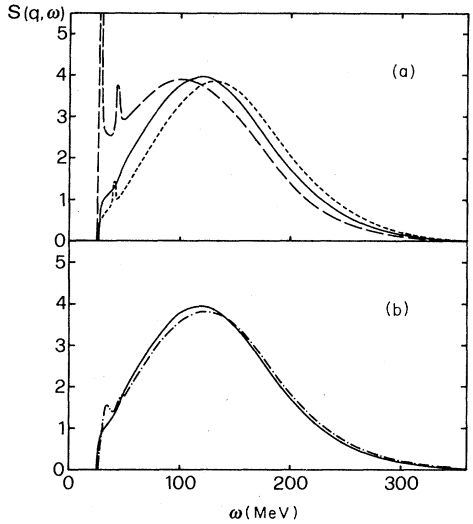

FIG. 3. Isoscalar (a) and longitudinal (b) response function for ^{12}C at constant momentum transfer $q=450$ MeV/c. Full line: independent-particle model; long dashed line: only direct term in particle-hole rescattering; short dashed line: only exchange term; dot-dashed line: both direct and exchange terms included. In the upper part of this figure the full and the short dashed lines are appropriate also for isovector response (the isovector direct contribution vanishes for a Wigner force).

direct and exchange particle-hole scattering for the isoscalar response, and Fig. 3(b) shows the total effect on the longitudinal (summed isoscalar and isovector) response. The total effect of particle-hole rescattering for this kinematics and for this particular choice of the residual interaction is very small. As can be seen from Fig. 3(a) this small net effect partly arises from a compensation of direct and exchange contributions. Both processes essentially give rise to a shift of the distribution in energy; for the attractive residual interaction (4.1), the direct process shifts the peak position of the isoscalar response towards low energies, while the exchange process has the opposite behavior. We use the nuclear matter response function to express this shift in the peak position in terms of the residual interaction and of the nucleon momentum distribution.

At momentum transfers larger than twice the Fermi momentum the single-particle nuclear matter polarization propagator $\Pi^0(q,\omega)$ is given by[8]

$$\Pi^0(q,\omega)=\frac{1}{2\pi^2}\frac{m}{q^3}\left\{qp_f m\omega_q+\tfrac{1}{2}[(qp_f)^2-(m\omega_q)^2]\times\ln\frac{m\omega_q^+ +qp_f}{m\omega_q^+ -qp_f}\right\}, \tag{4.2a}$$

where

$$\omega_q^+=\omega-\frac{q^2}{2m}+i\epsilon\ , \tag{4.2b}$$

and p_f is the Fermi momentum.

We expand $\Pi^0(q,\omega)$ in the energy ω around the free value $\omega=q^2/2m$:

$$\Pi^0(q,\omega)\approx\frac{mp_f^2}{4\pi q}\left\{\frac{4m}{\pi qp_f}\omega_q-i\left[1-\left[\frac{m}{qp_f}\right]^2\omega_q^2\right]\right\}. \tag{4.3}$$

We now use Eq. (3.15a) to estimate the first-order correction due to particle-hole rescattering. We find for the modification (assuming V to be real)

$$\begin{aligned}\mathrm{Im}\Pi^1(q,\omega)&=\mathrm{Im}(\Pi^0(q,\omega)\{1+[V(q)-\tfrac{1}{4}V_{\rm ex}(q,\omega)]\times\Pi^0(q,\omega)\}) \\ &\approx-\frac{mp_f^2}{4\pi q}\left\{1+2[V(q)-\tfrac{1}{4}V_{\rm ex}(q,\omega)]\times\frac{m^2p_f}{\pi^2q^2}\omega_q-\frac{m^2}{q^2p_f^2}\omega_q^2\right\}.\end{aligned} \tag{4.4}$$

At the quasielastic peak the single-particle response is purely imaginary and therefore, to this order, the particle-hole force simply shifts the peak position by the amount

$$\delta\omega=\frac{p_f^3}{\pi^2}[V(q)-\tfrac{1}{4}V_{\rm ex}(q,q^2/2m)]\ . \tag{4.5}$$

If we keep the direct piece only we find [cf. Eq. (3.3b)]

$$(\delta\omega)^D=\frac{4}{\pi}V_0\left[\frac{p_f}{\mu}\right]^3\frac{1}{1+q^2/\mu^2}\ , \tag{4.6}$$

which, for the parameters (4.1), the kinematics of Fig. 3 and with $p_f=220$ MeV/c takes the value

$$(\delta\omega)^D\approx-13\ \text{MeV}\ . \tag{4.7}$$

This is in quantitative agreement with our full finite-nucleus calculation [actually in practice at this kinematics the continued-fraction expansion (3.11a) already converges to the correct result after the first iteration].

In order to understand the influence of the exchange term we need evaluate the effective momentum transfer for this exchange process. As already emphasized, such effective momentum transfer is primarily determined by the nuclear Fermi motion rather than by the incident photon momentum.

We define the average momentum transfer in the exchange process by [cf. Eq. (3.15c)]

$$q_{\rm eff}^2(q,\omega)=\frac{\int d\mathbf{p}\,d\mathbf{k}\dfrac{(\mathbf{p}-\mathbf{k})^2}{\left[\omega_q^+-\dfrac{\mathbf{q}\cdot\mathbf{p}}{m}\right]\left[\omega_q^+-\dfrac{\mathbf{q}\cdot\mathbf{k}}{m}\right]}}{\int d\mathbf{p}\,d\mathbf{k}\dfrac{1}{\left[\omega_q^+-\dfrac{\mathbf{q}\cdot\mathbf{p}}{m}\right]\left[\omega_q^+-\dfrac{\mathbf{q}\cdot\mathbf{k}}{m}\right]}} \tag{4.8a}$$

which, evaluated at the quasielastic peak gives

$$q_{\rm eff}^2(q,q^2/2m)=p_f^2\left[1+\frac{32}{9\pi^2}\right]. \tag{4.8b}$$

With this value we obtain for the shift in the peak position due to the exchange process

$$(\delta\omega)^E = -\frac{1}{\pi} V_0 \left[\frac{p_f}{\mu}\right]^3 \frac{1}{1+q_{\rm eff}^2/\mu^2} , \tag{4.9a}$$

which yields [cf. Eq. (4.7)]

$$(\delta\omega)^E = +10 \text{ MeV} , \tag{4.9b}$$

which again agrees with our numerical calculation. The comparison with Eq. (4.7) makes explicit the almost complete cancellation for the particular case considered. The comparatively large effect of the exchange term despite the statistical suppression factor $\frac{1}{4}$ [cf. Eq. (4.5)] originates from the different kinematics of direct and exchange scattering, respectively. With increasing momentum of the incident photon, finite-range effects of the residual interaction suppress more and more the contribution of direct scattering [see Eq. (4.6)], while the effect of exchange scattering (at the quasielastic peak) is independent of the external momentum [Eqs. (4.8) and (4.9)]. Because of the very different kinematics of direct and exchange scattering processes, different properties of the residual interaction are important. In the actual finite-nucleus calculation of ^{12}C response, the evaluation of the direct process requires partial waves in the N-N interaction up to $L=11$—with the maximal contribution arising from $L=3$–4 ($q\langle r\rangle \approx 7$)—while the exchange process is determined by the N-N interaction in s, p, and d waves only, irrespective of the incident photon momentum.

So far our discussion has been focused on the isoscalar response with a spin-isospin independent residual force. We now include the isovector response in our discussion and use the more general form (3.3) of the residual interaction.

For this purpose we use, once more, the nuclear matter approximation to the response function. At the level of the one-doorway-state expression (3.15a), the inclusion of the spin-isospin exchange terms in the interaction is simple. Performing the appropriate spin-isospin sums the interaction $\tilde{V}(q)$ of Eq. (3.15b) is replaced for the isoscalar response by

$$\tilde{V}_0(q) = (a_0 + \tfrac{1}{2}a_1 + \tfrac{1}{2}a_2 + \tfrac{1}{4}a_3)V(q) - (\tfrac{1}{4}a_0 + \tfrac{1}{2}a_1 + \tfrac{1}{2}a_2 + a_3)V_{\rm ex}(q,\omega) , \tag{4.10a}$$

and for the isovector response by

$$\tilde{V}_1(q) = (\tfrac{1}{2}a_2 + \tfrac{1}{4}a_3)V(q) - (\tfrac{1}{4}a_0 + \tfrac{1}{2}a_1)V_{\rm ex}(q,\omega) . \tag{4.10b}$$

We note that in the isoscalar response all four terms of the interaction appear in both the direct and exchange terms, while in the isovector response the direct and exchange terms are affected only by those parts of the interaction which do or do not contain the isospin exchange operator, respectively. In the isovector response the incident photon creates a $T=1$ particle-hole state. "Direct" scattering [Fig. 2(b)] of this $T=1$ particle-hole state can occur only if the residual interaction is isospin-dependent; therefore only a_2 and a_3 appear in the direct term of $\tilde{V}_1(q)$. "Exchange" scattering, combined with the isospin exchange operator in the residual interaction, is, with respect to isospin, equivalent to direct scattering via an isospin-independent residual interaction. Thus only the terms a_0 and a_1 appear in the exchange term of $\tilde{V}_1(q)$.

For the particular case of the Wigner force already considered, only the exchange term contributes to the isovector response and, close to the quasielastic peak, it gives rise to the same repulsive shift of 10 MeV as in the exchange term of the isoscalar response [Eq. (4.9b)]. Thus, in the total longitudinal (summed isoscalar and isovector) response the small attractive shift of -3 MeV [cf. Eqs. (4.7) and (4.9)] in the isoscalar response cancels part of the repulsive shift in the isovector response. The net effect is a repulsive shift by a few MeV in agreement with the numerical results shown in Fig. 3(b).

The nuclear matter relations (4.10) make explicit the different effect of the residual interaction in the isoscalar and isovector response functions. This difference leads to differences between the longitudinal and transverse response functions, which contain isoscalar and isovector responses with different weights (cf. Appendix A). This feature is absent in the single-particle models where (apart from c.m. and Coulomb effects) the isoscalar and isovector responses are equal.

V. RESULTS

In Figs. 4–11 we present the results of our calculations for the longitudinal response function of ^{12}C at constant momentum transfers ranging from 200 to 550 MeV/c. The two curves in each figure correspond to the single-particle response function and to the response function including the particle-hole interaction, respectively.

The single-particle response is calculated with a phenomenological optical potential as in Ref. 3. As particle-hole interaction we have chosen the Kurath interaction[10,11] which is of the general form (3.3) with the following values of the parameters

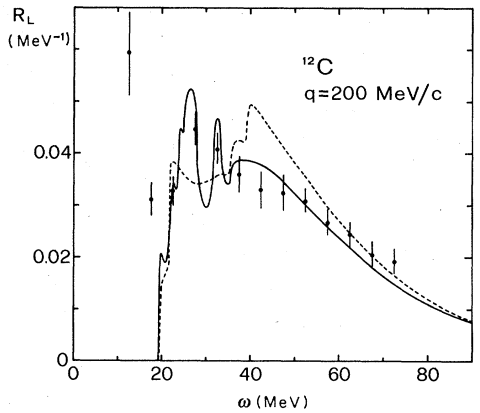

FIG. 4. Longitudinal response function of ^{12}C at constant momentum transfer $q=200$ MeV/c. The dashed line corresponds to the independent-particle model calculation, the full line shows the result of including particle-hole rescattering via the Kurath residual interaction (5.1). Data are from Ref. 7.

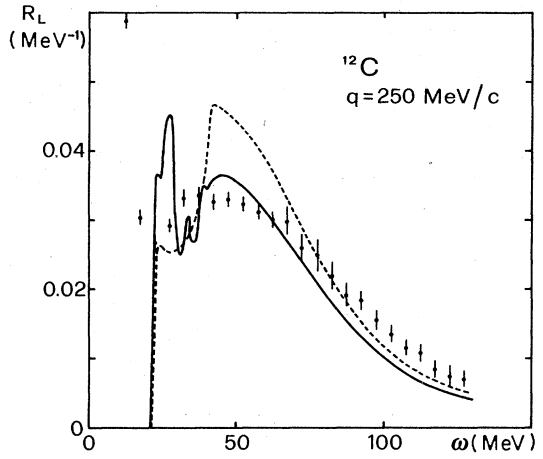

FIG. 5. Same as Fig. 4, $q=250$ MeV/c.

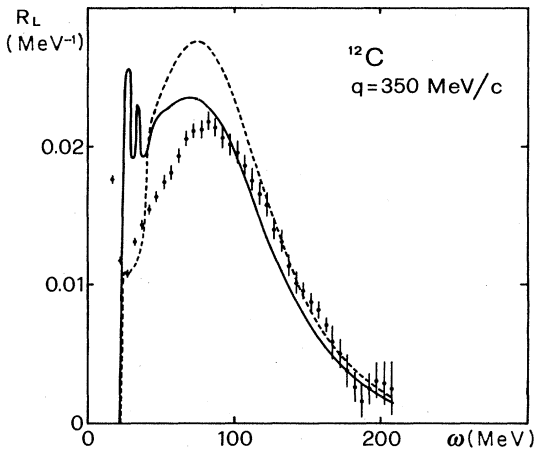

FIG. 7. Same as Fig. 4, $q=350$ MeV/c.

$$V_0=-36 \text{ MeV}, \quad \mu=0.714 \text{ fm}^{-1}, \qquad a_0=a_2=0, \quad a_1=\tfrac{1}{4}, \quad a_3=-1 . \tag{5.1}$$

The qualitative effect of this particular residual interaction is most easily seen in the nuclear matter approximation. From Eq. (4.10) we obtain,

$$\tilde{V}_0(q)=-\tfrac{1}{8}V(q)+\tfrac{7}{8}V_{\rm ex}(q,\omega) , \tag{5.2a}$$

$$\tilde{V}_1(q)=-\tfrac{1}{4}V(q)-\tfrac{1}{8}V_{\rm ex}(q,\omega) . \tag{5.2b}$$

Thus particle-hole rescattering in the isoscalar channel is dominated by the exchange process and the interaction is attractive. In the isovector channel the interaction is repulsive.

At the lower values of momentum transfer $q=200$–300 MeV/c, our calculations are in qualitative agreement with the experimental results. In particular, inclusion of the particle-hole rescattering process significantly improves the description by shifting strength from the quasielastic region $\omega\approx(q^2/2m)+\epsilon_s$ (ϵ_s is the separation energy ~ 20 MeV) into the resonance region around 20–30 MeV excitation energy and into the discrete excited states. This interplay of quasielastic, resonance, and discrete-state excitations is very important at these low momentum transfers. This is most clearly illustrated in Fig. 12 for the $L=2$ isoscalar excitation.

At $q=200$ MeV/c, the peak in the calculated response function at $\omega\approx 26$ MeV is due to an isoscalar quadrupole resonance with a total width of 4 MeV, which contributes up to 55% of the strength. This isoscalar resonance is superimposed on a rather broad isovector dipole excitation. Comparison with the single-particle response shows that the attractive residual interaction in the isoscalar channel shifts the quadrupole strength from the region above 30 MeV down in energy, and concentrates it to a large extent in this resonance. The depletion of the quadrupole single-particle strength above 30 MeV excitation energy due to particle-hole rescattering is of the order of 70% (see Fig. 12).

The peak at $\omega\approx 33$ MeV with a total width of about 2 MeV arises from an isovector dipole excitation. This resonance receives its main strength from energies around the threshold and from the discrete 1^- single-particle excitation which, with our choice of the single-particle potential, is located just below threshold at 17 MeV. This reversed effect of the residual interaction of course follows from the repulsive character of the particle-hole in-

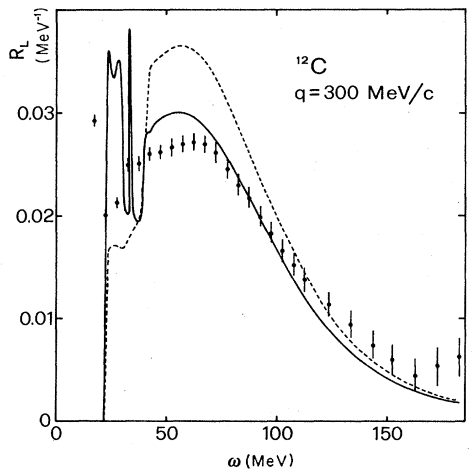

FIG. 6. Same as Fig. 4, $q=300$ MeV/c.

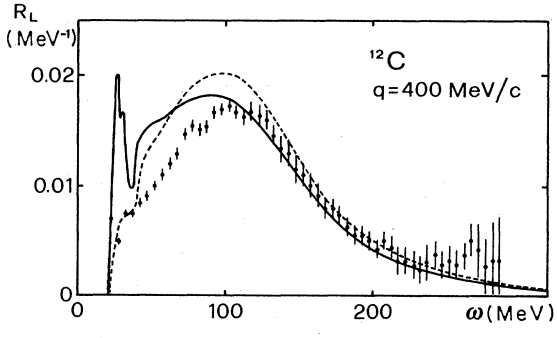

FIG. 8. Same as Fig. 4, $q=400$ MeV/c.

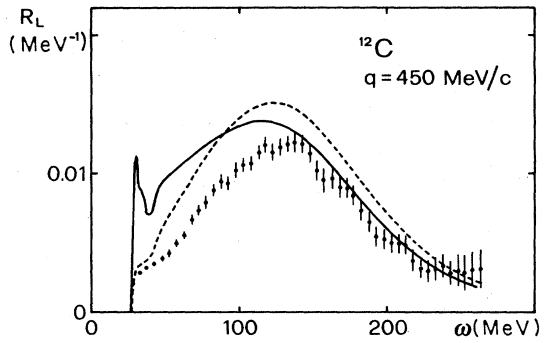

FIG. 9. Same as Fig. 4, $q = 450$ MeV/c.

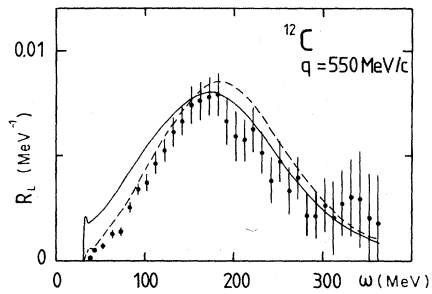

FIG. 11. Same as Fig. 4, $q = 550$ MeV/c.

teraction in the isovector channel.

In order to determine the amount of strength which has been shifted into the region of discrete excitations we have calculated the response function for complex energies $\omega + i\delta$. Thereby the sharp discrete excitation acquires a finite width. The value used for δ is 0.5 MeV.

In Fig. 13 we show the form factor calculated in this way for the 3^- $T=0$ excitation. With our choice of the particle-hole force this state is located at 13.5 MeV excitation energy, while the experimental value is 9.64 MeV. The comparison with the single-particle form factor exhibits the well-known enhancement due to particle-hole rescattering.[12] The agreement with the measured form factor is reasonable at low momentum transfer. At large momentum transfers apparently the effect of the particle-hole interaction (5.1) is too strong.

Analyzing the other discrete excitations ($L = 0,1,2$) in the same way, we can determine the fraction of the integrated single-particle response which has been shifted from the continuum part of the single-particle spectrum into the discrete excitations as a result of the particle-hole interaction. At the momentum transfer $q = 200$ MeV/c we find a depletion of the single-particle strength in the continuum by about 8%. The corresponding value at $q = 300$ MeV/c is 7%, and 5% at 400 MeV/c. As it can be expected, this shift in strength from the continuum to discrete excitations becomes less important with increasing momentum transfer.

We note that in our treatment of the residual interaction the energy integral of the response function is not changed, provided that the discrete excitations are properly taken into account. This result follows directly from completeness if the Hamiltonian is Hermitian. It can be generalized to energy-dependent complex interactions as follows. Consider the energy integral

$$\Sigma(q) = -\frac{1}{2i\pi}\,\mathrm{disc}\int_{\omega_{\mathrm{th}}}^{\infty} d\omega \langle 0 | O^{\dagger} \frac{1}{\omega^{+} - H} O | 0 \rangle \,, \tag{5.3}$$

with the shell-model ground state $|0\rangle$, the single-particle operator O of Eq. (2.2b), and the full many-body Hamiltonian H. The integral (5.3) can be written in the standard way as an integral along the upper and lower rim of the unitarity cut. This integration contour can be closed with a circle C_2 at infinity, starting at $\omega + i\epsilon$ and ending at $\omega - i\epsilon$. In this way we obtain

$$\Sigma(q) = \frac{1}{2i\pi}\int_{C_2} d\omega \langle 0 | O^{\dagger} \frac{1}{\omega - H} O | 0 \rangle - \sum_{\tilde{i}} | \langle \tilde{i} | O | 0 \rangle |^2 \,, \tag{5.4}$$

where the sum runs over the discrete eigenstates of the Hamiltonian H. In order to calculate the contribution from the circle C_2, we can replace the Hamiltonian H by any suitable model-Hamiltonian h since for any nonsingular interaction we expect the short time behavior of the Green's function, and, therefore, the large (complex) ω

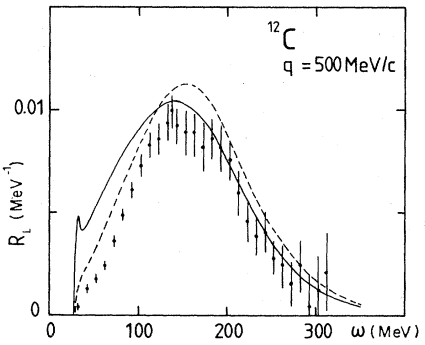

FIG. 10. Same as Fig. 4, $q = 500$ MeV/c.

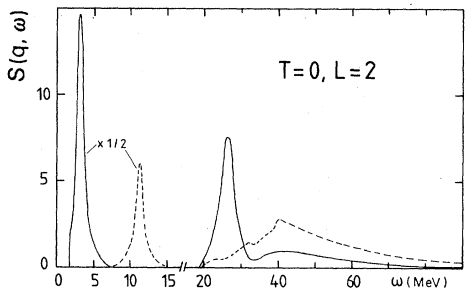

FIG. 12. Isoscalar quadrupole excitation in ^{12}C at constant $q = 200$ MeV/c. The short-dashed line gives the independent-particle model response, the full line gives the response including particle-hole rescattering. Note the change in scale at low energy. The two discrete peaks have been reduced by a factor of $\frac{1}{2}$ so the areas in the two parts of the figure are directly comparable.

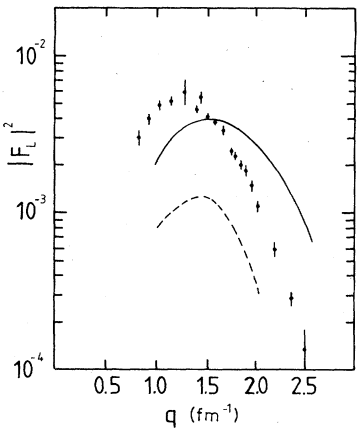

FIG. 13. Longitudinal form factor of the $T=0$, $L=3^-$ discrete excitation in ^{12}C. Dashed curve: independent-particle model; full curve: including residual interaction. Data are from Ref. 13.

behavior, to be controlled by the kinetic energy term in the Hamiltonian. In this way we can express $\Sigma(q)$ in terms of $\sigma(q)$, where $\sigma(q)$ is defined by (5.3) with H replaced by h:

$$\Sigma(q)=\sigma(q)-\sum_{\tilde{i}} |\langle \tilde{i}|O|0\rangle|^2+\sum_i |\langle i|O|0\rangle|^2 . \tag{5.5}$$

In deriving Eq. (5.5), we have performed the same contour deformations as in the preceding; this requires h to satisfy the relation

$$h^\dagger(\omega+i\epsilon)=h(\omega-i\epsilon) . \tag{5.6}$$

Equation (5.5) thus shows that the value of the sum rule

$$S(q)=\Sigma(q)+\sum_{\tilde{i}} |\langle \tilde{i}|O|0\rangle|^2 \tag{5.7}$$

is independent of the Hamiltonian used in the calculation of the intermediate states, provided that the corresponding Hamiltonian satisfies the relation (5.6).

Since the one-body operator O in Eq. (5.3) acts on the single-particle ground state $|0\rangle$, it can generate only 1p-1h states. Consequently, we can take for h either a single-particle Hamiltonian or the Hamiltonian including particle-hole interactions; according to (5.5), both choices lead to the same value of $S(q)$, provided the single-particle potential and the residual interaction satisfy the discontinuity condition (5.6).

Thus, particle-hole rescattering may lead to a redistribution of the transition strength, without changing, however, the total strength summed over both the discrete and continuum part of the excitation spectrum. Changes in the integrated strength are possible only if the ground state is a correlated rather than a pure single-particle state. We note however that in the presence of, for example, 2p-2h admixtures in the ground state, the intermediate states contributing to (5.3) cannot be restricted any more to the subspace of the 1p-1h states.

At the momentum transfers of 250 and 300 MeV/c, the data show appreciably less strength in the quasielastic region than predicted by the single-particle model. As at $q=200$ MeV/c, the particle-hole interaction reduces this strength of the quasielastic process, in qualitative agreement with experiment. However the data do not show concentration of this strength in the resonance region as predicted by the calculation. Furthermore, the strength at large energy losses is underestimated by our calculation. This is due partly to the effect of the attractive isoscalar interaction.

These deficiencies becomes even more pronounced at the higher momentum transfers 350, 400, and 450 MeV/c. At $q=400$ and 450 MeV/c the shape of the response function calculated in the single-particle model is actually in reasonable agreement with the data; however, as noticed in the Introduction, the strength at the peak is overestimated by 15—20% in this model. We note that the residual interaction again suppresses the strength at the high energy losses. This is in agreement with the data of 450 MeV/c, but in conflict with the data at 350 MeV/c. Moreover, the data again show no concentration of this strength at small energy losses as predicted by our calculation. This calculated shift of strength from large to small energy losses obtained for all the momentum transfers considered is not a particular feature of the interaction (5.1) used. Calculations with other parameterizations (Rosenfeld, Serber) of the residual interaction lead to similar results. As already noted, the interaction (5.1), as well as other forms of the residual interaction obtained from low-energy parametrizations, favors exchange processes in the particle-hole rescattering [cf. Eq. (5.2)]. We have seen in the previous section that the effect of these exchange processes on the response function is, in the peak region, approximately q independent [cf. Eq. (4.8)]. This is in contrast to the direct process which, due to the finite range of the interaction, becomes less important at higher momentum transfers. Actually in our calculation using a Wigner force of comparable strength (cf. Fig. 3), only minor modifications of the single-particle response at large q have been obtained. In particular, no concentration of the strength in the low energy region occurs with this interaction.

Thus the comparison with the data indicate that the particular residual interaction (5.1) is not adequate in the entire range of momentum transfers considered. This may not be surprising since this interaction has been obtained from the study of low-energy spectra. The longitudinal response data analyzed here rather favor a residual interaction with a weaker exchange and a stronger Wigner force. With such an interaction, the desired concentration of the strength into resonance and discrete state excitations at low momentum transfer can be preserved, while finite-range effects will cut down this unwanted shift of strength at high momentum transfer. By the same mechanism this would reduce the overestimate of the 3^- form factor at high momentum transfer as well.

However the major problem in reproducing the observed longitudinal response function cannot be solved in this way. With any form of the residual interaction, the energy integral of the response function must reproduce

the single-particle value which is too large in comparison to experiment. It is very difficult to imagine any form of realistic interaction which would shift strength from the quasielastic region by 150 MeV or more into the unobserved high energy-loss region.

Furthermore, we cannot see any reason for the energy dependence of the residual interaction to be so strong to resolve the discrepancy. One such possible source of energy dependence would be one-pion exchange in the residual interaction close to the pion production threshold. Although this mechanism can give rise to rapid energy variations of the transverse response, this will not be the case in the longitudinal response. Here, one-pion exchange can contribute only via the exchange process in particle-hole rescattering [diagram in Fig. 2(c)]. In the nuclear matter approximation (4.10) we have

$$\tilde{V}_0(q)\simeq\tilde{V}_1(q)\simeq\frac{q_{\rm eff}^2}{q_{\rm eff}^2+m_\pi^2}\ , \tag{5.8}$$

i.e., in the longitudinal response one-pion exchange cannot lead to either strong momentum-transfer dependence nor, via retardation effects, to strong energy dependence of the residual interaction. In the exchange process the energy and momentum-transfer dependences are always controlled by momenta of the order of p_f and by energies of the order of the hole binding energies.

More generally, we note that the energy dependence of the residual interaction is related to that of the optical potential. For instance, the lowest-order exchange contribution to the response function is obtained by hole-line exchange in the (particle) self-energy diagram, i.e., the exchange process in particle-hole rescattering corrects for the overcounting in the self-energy diagram which arises from identifying the ^{11}B optical potential with the ^{12}C optical potential. A similar argument applies to the direct process in particle-hole rescattering. Therefore any anomalously strong energy dependence in the residual interaction would most likely be in conflict with the known smooth energy dependence of the optical potential.

The same arguments already discussed also rule out the possibility of an imaginary part in the residual interaction strong enough and of appropriate sign to reduce substantially the response function in the quasielastic peak region.

In order to illustrate further this connection of the residual interaction with the optical potential we consider the process of particle-hole rescattering at very large energy and momentum transfers. In this case we can identify the residual interaction with the N-N scattering amplitude f at the appropriate energy. Assuming dominance of the direct term in N-N scattering at high energy [which corresponds to our exchange diagram of Fig. 2(c)] we have for the residual interaction at high energy:

$$V_0=-\frac{\mu^3}{2m}f(0)\ , \tag{5.9}$$

where $f(0)$ is the forward N-N scattering amplitude. Via the optical theorem the imaginary part of V_0 can be expressed in terms of the total cross section and of the nucleon momentum p:

$$\mathrm{Im}\,V_0=-\frac{\mu^3}{8\pi}\sigma_{\rm tot}\frac{p}{m}\ . \tag{5.10}$$

By using the nuclear matter approximation (4.4), it is seen that, to lowest order, the imaginary part in V_0 changes the height of the quasielastic peak without affecting its position.

At high momentum transfer $q\approx\sqrt{2m\omega}=p$, finite-range effects make the direct contribution negligible compared to the exchange contribution

$$\frac{1}{1+q^2/\mu^2}\ll\frac{1}{1+q_{\rm eff}^2/\mu^2} \tag{5.11}$$

and we obtain, therefore, for the relative change in the polarization propagator at the quasielastic peak

$$\frac{\delta\Pi}{\Pi}\approx\frac{1}{32\pi}\sigma_{\rm tot}p_f^2\frac{1}{1+q_{\rm eff}^2/\mu^2}\ . \tag{5.12}$$

With $\sigma_{\rm tot}\approx 43$ mb and $\mu=2$ fm^{-1} (corresponding to N-N scattering at an incident energy of 750 MeV) we obtain,

$$\frac{\delta\Pi}{\Pi}=+3.6\cdot10^{-2}\ . \tag{5.13}$$

Thus, in this high-energy approximation, the response is slightly increased by the imaginary part of the residual interaction. Evaluating in the same way the modification of the response due to the nucleon self-energy yields (cf. Ref. 3)

$$\left[\frac{\delta\Pi}{\Pi}\right]_{\text{self-energy}}\approx-\frac{1}{8\pi}\sigma_{\rm tot}p_f^2\ . \tag{5.14}$$

Apart from the finite-range reduction, Eqs. (5.14) and (5.12) just differ by a factor of 4. This shows explicitly the role of the particle-hole rescattering process as the hole-line exchange process of the nucleon self-energy. Finite-range effects do not occur in the self-energy correction which, in nuclear matter, is a zero momentum transfer process.

At the highest values of momentum transfer considered in our calculation, $q=500$ and 550 MeV/c, the disagreement between experimental data and the single-particle value of the longitudinal response function tends to decrease. Thus a particle-hole calculation with a Wigner-type force would also agree with experiment. The large concentration of the strength into the low-energy region predicted by the Kurath interaction is again due to the unreasonably large amount of exchange force in this parametrization.

Summarizing the discussion of our results we conclude that, within our treatment of the longitudinal response function, which takes into account particle self-energies via the optical potential and particle-hole rescattering in the Tamm-Dancoff approximation (TDA), it seems impossible to reproduce the observed longitudinal response in ^{12}C at large momentum transfer.

Obviously the discrepancy in this region of momentum transfer could still arise from more complicated many-body processes which have not been included in our treatment. Actually in calculations performed within the

framework of the random phase approximation (RPA), very good agreement has been obtained with the data at large momentum transfer.[14] The results of Ref. 14 therefore seem to indicate an important role of such more complicated processes even at momentum transfers as high as 400—500 MeV/c. However we note that in obtaining this agreement with the data the energy interval of the longitudinal response function has been reduced appreciably with respect to the single-particle value (by about 20% at 400 MeV/c). According to our previous discussion this large change in the integrated response indicates that ground-state RPA correlations included in this specific model are very important even at high momentum transfer. This result is very surprising; it may, however, be due to certain unrealistic aspects of the particular model adopted for the residual interaction. In the RPA of Ref. 14, the interaction used is a Skyrme force with a parameter set SK3.[15] The dominant terms in this interaction are given by

$$\langle \mathbf{k} \mid v_{12} \mid \mathbf{k}' \rangle \approx t_0(1+x_0P_\sigma)+\tfrac{1}{2}t_1(k^2+k'^2) , \quad (5.15)$$

where $\mathbf{k}$ and $\mathbf{k}'$ are the relative two-nucleon momenta. At $q \gg p_f$, we have approximately

$$k^2 \approx k'^2 \approx q^2/4 . \quad (5.16)$$

To estimate the effect of this force we use the nuclear matter Eqs. (4.10) and obtain for the effective interaction in the isoscalar channel

$$\tilde{V}_0(q)=\tfrac{3}{4}(t_0+\tfrac{1}{4}t_1q^2) , \quad (5.17)$$

which affects the response function in the same way as finite-range Wigner force of strength

$$\bar{V}_0=\frac{\mu^3}{4\pi}(1+q^2/\mu^2)(t_0+\tfrac{1}{4}t_1q^2) . \quad (5.18)$$

With the values of t_0 and t_1 used in Ref. 14, we find at $q=400$ MeV/c (with $\mu=0.7$ fm^{-1})

$$\bar{V}_0=-185 \text{ MeV} .$$

Thus probably the large effects found in Ref. 14 are due to the use of such a strong residual interaction.

Furthermore, we note the rapid momentum-transfer dependence of the effective interaction (5.18), arising from the momentum dependence of the interaction (5.15). Since the parameters t_0 and t_1 are of opposite sign, the two terms in (5.18) cancel each other at $q \approx 670$ MeV/c, i.e., the strength parameter $\bar{V}_0$ changes by 200 MeV if q changes from 400 to 700 MeV/c.

Thus these estimates indicate that the zero-range parametrization becomes unrealistic for momentum transfers appreciably larger than the Fermi momentum. The use of such a strong zero-range force for calculating the nuclear response at high momentum transfer apparently generates very large short-range components in the RPA correlations. However, explicit treatments of short-range correlations[16,17] show that neither the sum rule value nor the intensity at the quasielastic peak are modified by these correlations by more than 5%.

VI. SUMMARY

We have presented a calculation of the longitudinal response function of ^{12}C for momentum transfers ranging between 200 and 550 MeV/c. The calculation has been performed in the TDA, using a Green's function approach. The ingredients of our calculation are a phenomenological optical potential for evaluating the particle self-energy and a phenomenological finite-range residual interaction for evaluating particle-hole rescattering. We have applied a doorway-state method to the treatment of finite-range residual interactions. In this method the (interacting) response function is given in terms of a continued fraction, starting from its single-particle value. Our calculation treats quasielastic, resonance, and discrete state excitations on an equal footing. We have found rapid convergence of the doorway-state expansion in the various regions of the excitation spectrum.

As can be expected, the simultaneous treatment of the different types of excitations already mentioned is particularly important at low momentum transfers. We find at $q=200$—300 MeV/c large shifts of strength from the quasielastic region into the region of bound states and giant resonance as a result of particle-hole rescattering. These results are in reasonable agreement with experiment.

At large momentum transfers we find the standard "low energy" parametrizations of the residual interaction to be inadequate. In fact the large exchange components in the interaction shift, even at large momentum transfers, the strength towards lower excitation energy, in disagreement with the data.

At 400 and 450 MeV/c, calculations and data disagree in the energy-integrated strength. This disagreement is practically independent of the choice of the interaction, unless very strong repulsive residual interactions which would shift the strength into the unobserved high-energy region are allowed for. There is however no other evidence for such a strong repulsion.

Within a standard many-body description, the only way of possibly explaining the large deviations in the energy integrated response from the single-particle value is to include ground-state correlations. Because of the large momentum transfer involved, these correlations must modify the pair distribution function at distances of the order of 1 fm or less. However estimates of the effect of short-range correlations in quasielastic electron scattering do not indicate that such correlations are important enough to account for the discrepancy between experiment and the theoretical single-particle value.

ACKNOWLEDGMENTS

We are grateful to F. Malaguti for providing us with his bound-state Woods-Saxon code. F.A.B. thanks the Fondo Nacional de Desarollo Cyentifico y Tecnologico, Chile, and the Istituto Nazionale di Fisica Nucleare (INFN), Italy, for support. A.D. was supported by the INFN, Sezione di Firenze, Italy.

APPENDIX A

When comparing our calculations to experimental data we used the following definition of the longitudinal response function:

$$R_L(q,\omega)=\frac{G_E^2}{1+\frac{q_\mu^2}{4m^2}}\left[-\frac{1}{\pi}\mathrm{Im}\Pi_{\mathrm{is}}(q,\omega)-\frac{1}{\pi}\mathrm{Im}\Pi_{\mathrm{iv}}(q,\omega)\right] . \tag{A1}$$

Here, $q_\mu=(q,\omega)$ is the four-momentum transfer and G_E the electric nucleon form factor

$$G_E=\left[1+\frac{q_\mu^2}{18.24\ \mathrm{fm}^{-2}}\right]^{-2} . \tag{A2}$$

The polarization propagators Π_{is} and Π_{iv} are calculated with the isoscalar and isovector components, respectively, of the operator (2.2b).

At the quasielastic peak the definition (A1) agrees with the approximation in Eq. (17) of Ref. 3 for the unseparated cross section. Within the same approximation (i.e., neglect of convection current and spin-orbit terms) the following expression for the transverse response function can also be obtained:

$$R_T(q,\omega)\approx 2G_E^2\frac{q_\mu^2}{4m^2}\left\{(\mu_p+\mu_n)^2\left[-\frac{1}{\pi}\mathrm{Im}\Pi_{\mathrm{is}}(q,\omega)\right]+(\mu_p-\mu_n)^2\times\left[-\frac{1}{\pi}\mathrm{Im}\Pi_{\mathrm{iv}}(q,\omega)\right]\right\} . \tag{A3}$$

This approximation is valid only for large momentum transfer and for L-S closed shell nuclei.

We note that while the longitudinal response function (A1) at large momentum transfer has roughly equal isoscalar and isovector components, the transverse response function (A3) is almost entirely isovector since

$$[(\mu_p+\mu_n)/(\mu_p-\mu_n)]^2\approx 0.04 .$$

APPENDIX B

The description of the nucleus in terms of a mean potential field [Hartree-Fock (HF) or shell model] artificially binds the nuclear c.m. in an unphysical potential well. This violation of translation invariance can give rise to a spurious strength in the nuclear response which should be removed in order to get the intrinsic response. In this appendix we briefly illustrate the method followed here to correct, at least partially, the lack of translation invariance of the model used to calculate Π^0. Our approach is based on the following remarks:

(a) for the harmonic oscillator potential the c.m. problem can be solved exactly;

(b) the main spurious strength shows up in isoscalar dipole excitation.

To keep expressions as simple as possible, we consider a system of only four nucleons. The final result can be immediately extended to the case of A nucleons.

If we omit spin and isospin factors the g.s. wave function of ^{4}He in the harmonic oscillator model is

$$\psi_0=(\pi^{3/2}b^3)^{-A/2}\prod_i^A \exp[-x_i^2/(2b^2)] , \tag{B1}$$

where b is the oscillator parameter and $A=4$.

If we introduce the intrinsic coordinates $\mathbf{x}_i'$:

$$\mathbf{x}_i=\mathbf{X}+\mathbf{x}_i'$$

with

$$\mathbf{X}=\frac{1}{A}\sum_i^A \mathbf{x}_i ,$$

the wave function (B1) factorizes as

$$\psi_0=\psi_{\mathrm{c.m.}}\psi_{\mathrm{intr}}$$

with intrinsic wave function

$$\psi_{\mathrm{intr}}=(\pi^{3/2}b^3)^{-(A-1)/2}\exp\left[-\sum_i^A\frac{x_i'^2}{2b^2}\right] \tag{B2}$$

and c.m. wave function

$$\psi_{\mathrm{c.m.}}=(\pi^{3/2}b^3)^{-1/2}\exp\left[-\frac{AX^2}{2b^2}\right] . \tag{B3}$$

The translation-invariant wave function equivalent to (B1) may be written as

$$\psi_i=\frac{1}{\sqrt{V}}\int d\mathbf{y}\,\delta(\mathbf{y}-\mathbf{X})\exp(i\mathbf{K}\cdot\mathbf{y})\psi_{\mathrm{intr}} , \tag{B4}$$

where $\mathbf{K}$ is the c.m. momentum and V is the normalization volume for c.m. motion.

The intrinsic wave function (B2) can be further factorized into the product of a wave function describing the relative motion of, say, particle 1 with respect to the c.m. of the remaining $(A-1)$ particles so that Eq. (B4) gives

$$\psi_i=N\int d\mathbf{y}\,\delta(\mathbf{y}-\mathbf{X})\exp(i\mathbf{K}\cdot\mathbf{y})\varphi_i(\mathbf{x}_1-\mathbf{Y})\psi_{A-1} , \tag{B5}$$

where N is the appropriate normalization factor,

$$\mathbf{Y}=\frac{1}{A-1}\sum_{j\neq 1}\mathbf{x}_j$$

is the c.m. coordinate of the $(A-1)$ cluster,

$$\varphi_i(\mathbf{x}_i-\mathbf{Y})=\exp\left[-\frac{A-1}{A}\frac{(\mathbf{x}_1-\mathbf{Y})^2}{2b^2}\right] \tag{B6}$$

is the (unnormalized) wave function describing the relative motion of particle 1 with respect to the cluster of the remaining $(A-1)$ particles, and

$$\psi_{A-1}=\exp\left[-\sum_{i\neq 1}\frac{(\mathbf{x}_i-\mathbf{Y})^2}{2b^2}\right] \tag{B7}$$

describes the $(A-1)$ cluster.

We note that the wave function (B6) is a solution of the Schrödinger equation with a reduced mass $\mu=[(A-1)/A]m$.

Of course the factorization (B5) is exact only for the harmonic oscillator. However, since for light nuclei more realistic single-particle ground-state (g.s.) wave functions are rather well approximated by harmonic oscillator wave functions, it is reasonable to replace (B6) with a more realistic (in our case Woods-Saxon) wave function. Of course, such a wave function should be a solution of the Schrödinger equation with a reduced mass μ.

Now we *assume* that the factorization (B5) holds true also after that particle 1 has absorbed an external photon, thus we write for the resulting nuclear excited state

$$\psi_f = N' \int d\mathbf{y}\, \delta(\mathbf{y}-\mathbf{X}) \exp(i\mathbf{K}'\cdot\mathbf{y}) \varphi_f(\mathbf{x}_1-\mathbf{Y}) \psi_{A-1} . \quad \text{(B8)}$$

Here, N' is the appropriate normalization factor, φ_f is the wave function describing the excited relative motion of particle 1, and ψ_{A-1} always describes the $(A-1)$ cluster, which in this model has been assumed to remain unchanged in the process.

The assumption (B8) clearly is not exact even for harmonic oscillator wave functions; however, rather than worrying about the neglected terms, we shall check it at the end by comparing the exact result with the consequences of approximation (B8).

In Coulomb excitation the transition matrix element for the absorption of an external photon of momentum $\mathbf{q}$ by particle 1 will be

$$t_{fi} = \langle \psi_f \,|\, \exp(i\mathbf{q}\cdot\mathbf{x}_1) \,|\, \psi_i \rangle$$
$$= NN' \int d\mathbf{y} \exp[i(\mathbf{K}-\mathbf{K}')\cdot\mathbf{y}] \int d\mathbf{z} \int d\mathbf{x}_1 \cdots d\mathbf{x}_A \delta(\mathbf{y}-\mathbf{X}) \delta(\mathbf{z}-\mathbf{Y}) \varphi_f^*(\mathbf{x}_1-\mathbf{z}) \varphi_i(\mathbf{x}_1-\mathbf{z}) \exp(i\mathbf{q}\cdot\mathbf{x}_1) \,|\, \psi_{A-1} \,|^2 . \quad \text{(B9)}$$

We introduce coordinates with respect to the c.m. of the $(A-1)$ cluster,

$$\mathbf{y}_i = \mathbf{x}_i - \mathbf{Y} = \mathbf{x}_i - \mathbf{z} , \quad \text{(B10)}$$

then

$$\delta(\mathbf{z}-\mathbf{Y}) = (A-1)^3 \delta\left[\sum_{j\neq 1} \mathbf{y}_j \right]$$

and

$$\delta(\mathbf{y}-\mathbf{X}) = \delta\left[\mathbf{y} - \mathbf{z} - \frac{1}{A}\mathbf{y}_1 \right] .$$

Now we can replace the integration variables $\mathbf{x}_i$ in (B9) by the new coordinates $\mathbf{y}_i$. Then integration over the cluster coordinates $\mathbf{y}_2 \cdots \mathbf{y}_A$ gives just a number; in our case, using (B7) we get

$$\int d\mathbf{y}_2 \cdots d\mathbf{y}_A \delta\left[\sum_{j\neq 1} \mathbf{y}_j \right] \,|\, \psi_{A-1} \,|^2 = \left[\frac{\pi b^2}{\sqrt{3}} \right]^3 .$$

The integration over the variable $\mathbf{y}$ gives the correct overall momentum conservation, and we obtain

$$t_{fi} = NN'(A-1)^3 \left[\frac{\pi b^2}{\sqrt{3}} \right]^3 (2\pi)^3 \delta(\mathbf{K}+\mathbf{q}-\mathbf{K}')$$
$$\times \int d\mathbf{y}_1 \varphi_f^*(\mathbf{y}_1) \exp(i\mathbf{q}'\cdot\mathbf{y}_1) \varphi_i(\mathbf{y}_1) \quad \text{(B11)}$$

with $\mathbf{q}' = [(A-1)/A]\mathbf{q}$. That is, in order to calculate the desired transition matrix element, in our approximation we still need to evaluate only a single-particle matrix element, but in terms of relative-motion wave functions and with an effective reduced momentum transfer.

Of course we also have to consider the amplitude for the process in which the external photon couples to the particles in the $(A-1)$ cluster. If we do this then we are led to calculation of transition matrix elements similar to (B9) but with, say, $\exp(i\mathbf{q}\cdot\mathbf{x}_2)$ replacing the quantity $\exp(i\mathbf{q}\cdot\mathbf{x}_1)$. Denoting this matrix element by $\tilde{t}_{fi}$, we have

$$\tilde{t}_{fi} = NN'(A-1)^3 (\sqrt{3}\pi b^2)^3 (2\pi)^3 \delta(\mathbf{K}+\mathbf{q}-\mathbf{K}')$$
$$\times F_{A-1}(q) \int d\mathbf{y}_1 \varphi_f^*(\mathbf{y}_1) \exp\left[-i\frac{\mathbf{q}\cdot\mathbf{y}_1}{A} \right] \varphi_i(y_1) , \quad \text{(B12)}$$

where $F_{A-1}(q)$ is the intrinsic form factor of the $(A-1)$ cluster normalized to 1 when $q \to 0$. In our example (^{4}He with harmonic oscillator wave functions),

$$F_{A-1}(q) = \exp(-q^2 b^2/6) .$$

The matrix elements t_{fi} and $\tilde{t}_{fi}$ must be taken in different combinations, depending on the process considered. For example, for isoscalar response we need to take

$$t_{fi} + (A-1)\tilde{t}_{fi} ,$$

while for isoscalar response

$$t_{fi} - \tilde{t}_{fi}$$

is the right combination.

We can reassume our prescription for c.m. correction in Coulomb scattering as follows.

When calculating the isoscalar amplitude replace the single-particle [shell model (SM)] matrix element

$$\langle \varphi_f^{\mathrm{SM}}(\mathbf{x}_1) \,|\, \exp(i\mathbf{q}\cdot\mathbf{x}_1) \varphi_i^{\mathrm{SM}}(x_1) \rangle \quad \text{(B13)}$$

by the matrix element

$$\langle \varphi_f(\mathbf{y}_1) \,|\, \exp(i\mathbf{q}'\cdot\mathbf{y}_1) + (A-1) F_{A-1}(q) \times \exp\left[-i\frac{\mathbf{q}\cdot\mathbf{y}_1}{A} \right] \,|\, \varphi_i(\mathbf{y}_1) \rangle ; \quad \text{(B14)}$$

when calculating the isovector amplitude, replacing the single-particle matrix element (B13) by

$$\langle \varphi_f(\mathbf{y}_1) \,|\, \exp(i\mathbf{q}'\cdot\mathbf{y}_1) - F_{A-1}(q) \exp\left[-i\frac{\mathbf{q}\cdot\mathbf{y}_1}{A} \right] \,|\, \varphi_i(\mathbf{y}_1) \rangle .$$

In other words, the one-body operator $\exp(i\mathbf{q}\cdot\mathbf{x}_1)$ should be replaced by the effective one-body operator

$$\exp\left[i\frac{A-1}{A}\mathbf{q}\cdot\mathbf{y}_1\right]+\delta F_{A-1}(q)\exp\left[-i\frac{\mathbf{q}}{A}\cdot\mathbf{y}_1\right]$$

with

$$\delta=\begin{cases}A-1 & \text{isoscalar response}\\ -1 & \text{isovector response,}\end{cases}$$

while the shell-model single-particle wave function should be replaced by the corresponding relative-motion wave function $\varphi(\mathbf{y}_1)$[φ^{SM} is a solution of the Schrödinger equation with the full nucleon mass m, while φ is a solution of the Schrödinger equation with reduced mass $\mu=((A-1)/A)m$].

It can be easily checked that for harmonic oscillator wave functions the above-mentioned prescription gives the exact intrinsic elastic form factor. Moreover, the effective operator in (B14) always vanishes in the long-wavelength limit, thus giving no spurious isoscalar dipole excitation.

For the harmonic oscillator, we can also compare our procedure with the exact calculation. In Fig. 14 we compare the intrinsic response given by the prescription with the exact response[18] and with the shell-model (no c.m. correction) response. It can be seen that in spite of some discrepancies in the low-energy limit, on the whole the prescription does rather well. For this reason we feel confident in applying it also to our Woods-Saxon calculation.

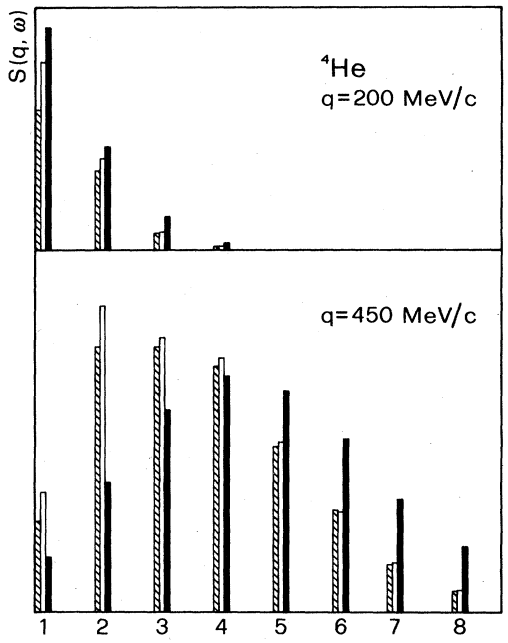

FIG. 14. Intrinsic longitudinal response for ^{4}He in the harmonic oscillator model; black: no c.m. correction, white: present prescription, shaded: exact. The energy loss is in units of $\hbar\omega$.

APPENDIX C

In order to include the c.m. correction and the isospin dependence of the transition operator, the expressions (3.17) of the doorway states are modified according to the replacement $j_L(qr)\to a_L$, where the quantity a_L is given by (see Appendix B)

$$a_L=j_L\left[\frac{A-1}{A}qr\right]+(-)^L(A-1)F_{A-1}(q)j_L\left[\frac{1}{A}qr\right] \tag{C1a}$$

for isoscalar response, and by

$$a_L=\tau^3\left[j_L\left[\frac{A-1}{A}qr\right]-(-)^L F_{A-1}(q)j_L\left[\frac{1}{A}qr\right]\right] \tag{C1b}$$

for isovector response. Moreover the hole wave function $u_i(r)$ has to be a solution of the radial Schrödinger equation with reduced mass μ.

In order to give the partial-wave decomposition of the exchange operator (3.19) for the general residual interaction (3.3a), we introduce the following radial quantities corresponding to the direct and exchange term, respectively:

$$\mathscr{D}^{ji}_{\beta\alpha}(r',r)=\int d\hat{\mathbf{r}}\,d\hat{\mathbf{r}}'[\mathscr{Y}^{m_\beta}_{j_\beta l_\beta}(\hat{\mathbf{r}}')]^\dagger\langle j^{-1}\,|\,\langle\tau_\beta|\,\Delta(\mathbf{r}',\mathbf{r})\,|\,\tau_\alpha\rangle\,|\,i^{-1}\rangle\mathscr{Y}^{m_\alpha}_{j_\alpha l_\alpha}(\hat{\mathbf{r}})\,, \tag{C2a}$$

$$\mathscr{E}^{ji}_{\beta\alpha}(r',r)=\int d\hat{\mathbf{r}}'\,d\hat{\mathbf{r}}[\mathscr{Y}^{m_\beta}_{j_\beta l_\beta}(\hat{\mathbf{r}}')]^\dagger\langle j^{-1}\,|\,\langle\tau_\beta|\,E(\mathbf{r}',\mathbf{r})\,|\,\tau_\alpha\rangle\,|\,i^{-1}\rangle\mathscr{Y}^{m_\alpha}_{j_\alpha l_\alpha}(\hat{\mathbf{r}})\,. \tag{C2b}$$

Rather than the explicit expressions for the quantities $\mathscr{D}$ and $\mathscr{E}$, we give the following linear combinations which arise when performing the angular integrations:

$$\sum_{\substack{m_j\\ m_\beta}} R^{LM}_{\beta j}\mathscr{D}^{ji}_{\beta\alpha}(r',r)=4\pi\int_0^\infty dx\frac{1}{r'}g^{j_\beta l_\beta}(r',x,\omega_j)u_j(x)\frac{u_i(r)}{r}v_L(x,r)$$

$$\times\{\delta_{\tau_\alpha\tau_i}\delta_{\tau_\beta\tau_j}[a_0+\tfrac{1}{2}a_1F_L(\beta,j,\alpha,i)]+\delta_{\tau_\alpha\tau_\beta}\delta_{\tau_i\tau_j}[a_2+\tfrac{1}{2}a_3F_L(\beta,j,\alpha,i)]\}A_2(L,\beta,j)R^{LM}_{\alpha i} \tag{C3a}$$

and

$$\sum_{\substack{m_j \\ m_\beta}} R_{\beta j}^{LM} \mathscr{E}_{\beta\alpha}^{ji}(r',r) = 4\pi \frac{1}{rr'} g^{j_\beta l_\beta}(r',r,\omega_j) \int_0^\infty dx\, u_j(x) u_i(x) \sum_l v_l(x,r)$$

$$\times \{ \delta_{\tau_\alpha \tau_\beta} \delta_{\tau_i \tau_j} [a_0 A_3(L,l,\beta,j,\alpha,i) + a_1 A_4(L,l,\beta,j,\alpha,i)] + \delta_{\tau_\alpha \tau_i} \delta_{\tau_\beta \tau_j}$$

$$\times [a_2 A_3(L,l,\beta,j,\alpha,i) + a_3 A_4(L,l,\beta,j,\alpha,i)] \} R_{\alpha i}^{LM} , \tag{C3b}$$

where the coefficients A_2, A_3, A_4, and F_L are defined as follows [see Eqs. (3.21)]:

$$\sum_{\substack{m_i \\ m_\alpha}} R_{\alpha i}^{lm} R_{\alpha i}^{LM} = \delta_{l,L} \delta_{m,M} A_2(L,\alpha,i) , \tag{C4}$$

$$\sum_{\substack{m_i m_\alpha \\ m}} R_{ij}^{lm} R_{\alpha\beta}^{lm} R_{\alpha i}^{LM} = A_3(L,l,\alpha,i,\beta,j) R_{\beta j}^{LM} , \tag{C5}$$

$$A_4(L,l,\beta,j,\alpha,i) = (-)^{l+L}(2l+1) \begin{Bmatrix} l_\alpha & l_i & L \\ l_j & l_\beta & l \end{Bmatrix} \frac{\begin{bmatrix} l_j & l_i & l \\ 0 & 0 & 0 \end{bmatrix} \begin{bmatrix} l_\alpha & l_\beta & l \\ 0 & 0 & 0 \end{bmatrix}}{\begin{bmatrix} l_\beta & l_j & L \\ 0 & 0 & 0 \end{bmatrix} \begin{bmatrix} l_\alpha & l_i & L \\ 0 & 0 & 0 \end{bmatrix}} A_2(L,\beta,j) , \tag{C6}$$

$$F_L(\beta,j,\alpha,i) = 1 + (1-\delta_{L,0}) \frac{[l_i(l_i+1) - l_\alpha(l_\alpha+1) - j_i(j_i+1) + j_\alpha(j_\alpha+1)][l_j(l_j+1) - l_\beta(l_\beta+1) - j_j(j_j+1) + j_\beta(j_\beta+1)]}{L(L+1)} . \tag{C7}$$

Both the coefficients A_3 and A_4 should be taken to be zero if the denominators happen to vanish.

---

*Permanent address: Dipartimento di Fisica, Università degli Studi di Firenze, Firenze, Italy.

†Permanent address: Departamento de Fisica, Universidad de Chile, Santiago, Chile.

[1]R. R. Whitney, I. Sick, F. R. Ficenec, R. D. Kephart, and W. P. Thrower, Phys. Rev. C 9, 2230 (1974).

[2]P. Barreau *et al.*, Nucl. Phys. **A402**, 515 (1983).

[3]Y. Horikawa, F. Lenz, and N. C. Mukhopadhyay, Phys. Rev. C 22, 1680 (1980).

[4]G. Do Dang and Pham Van Thieu, Phys. Rev. C 28, 1845 (1983).

[5]J. V. Noble, Phys. Rev. Lett. **46**, 412 (1981).

[6]Z. E. Meziani *et al.*, Phys. Rev. Lett. **52**, 2130 (1984).

[7]P. Barreau *et al.*, Commissariat a l'Energie Atomique, France, Report CEA-N-2334, 1983 (unpublished).

[8]A. L. Fetter and J. D. Walecka, *Quantum Mechanics of Many-Particle Systems* (McGraw-Hill, New York, 1971).

[9]F. Lenz, E. J. Moniz, and K. Yazaki, Ann. Phys. (N.Y.) **129**, 84 (1980).

[10]A. de Shalit and H. Feshbach, *Theoretical Nuclear Physics* (Wiley, New York, 1974).

[11]D. Kurath, Phys. Rev. **101**, 216 (1956).

[12]V. Gillet and A. Melkanoff, Phys. Rev. **133**, B1190 (1964).

[13]H. Crannell, Phys. Rev. **148**, 1107 (1966).

[14]M. Cavinato, D. Drechsel, E. Fein, M. Marangoni, and A. M. Saruis, Nucl. Phys. **A423**, 376 (1984).

[15]D. Vautherin and D. M. Brink, Phys. Rev. C 5, 626 (1972).

[16]C. Ciofi degli Atti, in *The Structure of Nuclei* (IAEA, Vienna, 1972).

[17]F. Dellagiacoma, R. Ferrari, G. Orlandini, and M. Traini, Phys. Rev. C **29**, 777 (1984).

[18]A. Dellafiore and M. Traini, Nucl. Phys. **A344**, 509 (1980).